

η, η' photoproduction and electroproduction off protons

B. Borasoy, E. Marco, S. Wetzel

*Physik Department -T39, TU München,
85747 Garching, Germany*

Abstract

Photo- and electroproduction of η, η' mesons on protons are investigated within a relativistic chiral unitary approach based on coupled channels. The s wave potentials for electroproduction and meson-baryon scattering are derived from a chiral effective Lagrangian which includes the η' as an explicit degree of freedom and incorporates important features of the underlying QCD Lagrangian such as the axial $U(1)$ anomaly. The effective potentials are iterated in a Bethe-Salpeter equation and cross sections for η, η' photo- and electroproduction from protons are obtained. The results for the η' photoproduction cross section reproduce the appearance of an S_{11} resonance around 1.9 GeV observed at ELSA. The inclusion of electromagnetic form factors increases the predicted η electroproduction cross sections, providing a qualitative explanation for the hard form factor of the photocoupling amplitude observed at CLAS.

1 Introduction

Photoproduction of mesons is a tool to study baryon resonances and the investigation of transitions between these states provides a crucial test for hadron models. Because of their hadronic decay modes nucleon resonances have large overlapping widths, which makes it difficult to study individual states, but selection rules in certain decay channels can reduce the number of possible resonances. The isoscalars η and η' are such examples since – due to isospin conservation – only the isospin- $\frac{1}{2}$ excited states decay into the ηN and $\eta' N$ channels. Electroproduction experiments are even more sensitive to the structures of the nucleon due to the longitudinal coupling of the virtual photon to the nucleon spin and might in addition yield some insight into a possible onset of perturbative QCD.

In this work, we restrict ourselves to the low-energy region where non-perturbative QCD dominates. Chiral symmetry is believed to govern interactions among hadrons at low energies where the relevant degrees of freedom are

not the quark and gluon fields of the QCD Lagrangian, but composite hadrons. In order to make contact with experiment one must resort to non-perturbative methods such as chiral effective field theory which incorporates the symmetries and symmetry breaking patterns of the underlying theory QCD and is written in terms of the active degrees of freedom. A systematic loop expansion can be carried out in the framework of chiral perturbation theory (ChPT) which inherently involves a characteristic scale $\Lambda_\chi = 4\pi F_\pi \approx 1.2$ GeV at which the chiral series is expected to break down. The limitation to very low-energy processes is even enhanced in the vicinity of resonances. The appearance of resonances in certain channels constitutes a major problem to the loopwise expansion of ChPT, since their contribution cannot be reproduced at any given order of the chiral series. Recently, considerable effort has been undertaken to combine the chiral effective Lagrangian approach with the Bethe-Salpeter equation making it possible to go to energies beyond Λ_χ and to generate the resonances dynamically [1]. Two prominent examples of resonances in the baryonic sector are the $\Lambda(1405)$ and the $S_{11}(1535)$.

The η' is closely related to the axial $U(1)$ anomaly. The QCD Lagrangian with massless quarks exhibits an $SU(3)_L \times SU(3)_R$ chiral symmetry which is broken down spontaneously to $SU(3)_V$, giving rise to a Goldstone boson octet of pseudoscalar mesons which become massless in the chiral limit of zero quark masses. On the other hand, the axial $U(1)$ symmetry of the QCD Lagrangian is broken by the anomaly which manifests itself phenomenologically in the mass of the $\eta'(958)$ which is considerably heavier than the masses of the (pseudo-) Goldstone bosons.

The experimental data for η' photoproduction from ELSA [2] suggested the coherent excitation of two resonances $S_{11}(1897)$ and $P_{11}(1986)$. In this work we will restrict ourselves to s waves and therefore the comparison with data should only be valid in the near threshold region. One of the purposes of this work is to shed some light on the s wave resonance $S_{11}(1897)$. Furthermore, this investigation will provide a test whether processes up to energies of $\sqrt{s} \sim 2$ GeV are still constrained by chiral symmetry and whether the η' meson can be included in the effective Lagrangian with baryons as proposed in [3].

2 Sketch of the calculation

In this section we briefly outline the calculation. In the first part, features of the effective Lagrangian are presented, while in the second part the coupled channel approach is introduced and then generalized to photo- and electroproduction processes.

2.1 The effective $U(3)$ Lagrangian

In the effective field theory one constructs the most general Lagrangian with the same symmetries as the underlying theory QCD. In order to include the pseudoscalar singlet field η_0 , $SU(3)_L \times SU(3)_R$ chiral symmetry of conventional ChPT is extended to $U(3)_L \times U(3)_R$ by treating the QCD vacuum angle θ as an external field which compensates the axial $U(1)$ anomaly [3, 4].

The pseudoscalar meson nonet is summarized in a unitary matrix $U \in U(3)$

$$U(\phi, \eta_0) = u^2(\phi, \eta_0) = \exp \left(i \frac{\sqrt{2}}{f_\pi} \phi + i \sqrt{\frac{2}{3}} \frac{\eta_0}{f_\pi} \right), \quad (1)$$

where $f_\pi \simeq 92.4$ MeV is the pion decay constant and ϕ contains the Goldstone bosons (π, K, η_8) . The ground state baryon octet $(N, \Lambda, \Sigma, \Xi)$ is also collected in a 3×3 matrix and the effective Lagrangian is a function of U , B and their derivatives, $\mathcal{L} = \mathcal{L}(U, \partial U, \partial^2 U, \dots, B, \partial B, \dots, \mathcal{M}, \frac{\sqrt{6}}{f_\pi} \eta_0 + \theta)$, with $\mathcal{M} = \text{diag}(m_u, m_d, m_s)$ being the quark mass matrix and θ the QCD vacuum angle which appears in the gauge invariant combination with the singlet field η_0 .

The $U(3)_L \times U(3)_R$ chiral effective Lagrangian of the pseudoscalar meson nonet coupled to the ground state baryon octet can be decomposed as

$$\mathcal{L} = \mathcal{L}_M + \mathcal{L}_{MB} \quad (2)$$

with the mesonic piece up to second chiral order [5]

$$\mathcal{L}_M = -\frac{v_0}{f_\pi^2} \eta_0^2 + \frac{f_\pi^2}{4} \langle u_\mu u^\mu \rangle + \frac{f_\pi^2}{4} \langle \chi_+ \rangle + i \frac{v_3}{f_\pi} \eta_0 \langle \chi_- \rangle, \quad (3)$$

where $\langle \dots \rangle$ denotes the trace in flavor space. The object $u_\mu = iu^\dagger \nabla_\mu U u^\dagger$ contains the covariant derivative of the meson fields

$$\nabla_\mu U = \partial_\mu U + ie\mathcal{A}_\mu [Q, U] \quad (4)$$

with $Q = \frac{1}{3}\text{diag}(2, -1, -1)$ being the quark charge matrix and \mathcal{A}_μ the photon field. Explicit chiral symmetry breaking is induced via the quark mass matrix \mathcal{M} which enters in the combinations $\chi_\pm = 2B_0(u^\dagger \mathcal{M} u^\dagger \pm u \mathcal{M} u)$ with $B_0 = -\langle 0|\bar{q}q|0 \rangle/f_\pi^2$ the order parameter of spontaneous symmetry violation.

The second and third term of Eq. (3) appear already in conventional $SU(3)$ ChPT whereas the first and fourth one are due to the axial $U(1)$ anomaly. The first one is the mass term of the singlet field η_0 which remains in the chiral limit of vanishing quark masses. The coefficient v_0 is a parameter not fixed by

chiral symmetry and in the large N_c limit it is proportional to the topological susceptibility of Gluodynamics. The fourth term contributes to η_8 - η_0 mixing.

The meson-baryon interactions are collected in $\mathcal{L}_{\phi B}$ which reads at lowest chiral order [3]

$$\begin{aligned}\mathcal{L}_{MB}^{(1)} = & i\langle\bar{B}\gamma_\mu[D^\mu, B]\rangle - \overset{\circ}{M}\langle\bar{B}B\rangle + iu_1\frac{\eta_0^2}{f_\pi^2}\left(\langle[D^\mu, \bar{B}]\gamma_\mu B\rangle - \langle\bar{B}\gamma_\mu[D^\mu, B]\rangle\right) \\ & - \frac{1}{2}D\langle\bar{B}\gamma_\mu\gamma_5\{u^\mu, B\}\rangle - \frac{1}{2}F\langle\bar{B}\gamma_\mu\gamma_5[u^\mu, B]\rangle - \frac{1}{2}D_s\langle\bar{B}\gamma_\mu\gamma_5B\rangle\langle u^\mu\rangle,\end{aligned}\quad (5)$$

where only the terms that are necessary for the present calculation are kept and the superscript denotes the chiral order. $\overset{\circ}{M}$ is the common baryon octet mass in the chiral limit, D, F, D_s are the axial vector couplings of the mesons to the baryons and D_μ is the covariant derivative of the baryon fields. Terms from $\mathcal{L}_{MB}^{(2)}$ are also included in the calculation, but are not shown here for brevity, *cf.* [6] for details.

2.2 The coupled channel approach

First, the s wave interaction kernel V of meson-baryon scattering is extracted from the contact and s -channel Born terms. Unitarity imposes a restriction on the T -matrix

$$T^{-1} = V^{-1} + G,\quad (6)$$

where G is the scalar meson baryon loop integral

$$G(q^2) = \int \frac{d^d l}{(2\pi)^d} \frac{i}{[(q-l)^2 - M_B^2 + i\epsilon][l^2 - m_\phi^2 + i\epsilon]}\quad (7)$$

with $\text{Im } G = \text{Im } T^{-1}$, and we have approximated the remaining real part in Eq. (6) by V^{-1} . Matrix inversion of Eq. (6) yields the Bethe-Salpeter equation

$$T = [1 + V \cdot G]^{-1} \cdot V\quad (8)$$

which is equivalent to the summation of a bubble chain.

This approach is readily extended to electroproduction of mesons on baryons. The electric dipole amplitude B_0^+ and the longitudinal s wave C_0^+ at the tree level are derived from the contact and Born terms of meson electroproduction and inserted into the meson-baryon bubble chain, in order to obtain the *full* electric dipole amplitude E_0^+ and longitudinal s wave L_0^+ , respectively,

$$E_0^+ = [1 + V \cdot G]^{-1} \cdot B_0^+, \quad L_0^+ = [1 + V \cdot G]^{-1} \cdot C_0^+, \quad (9)$$

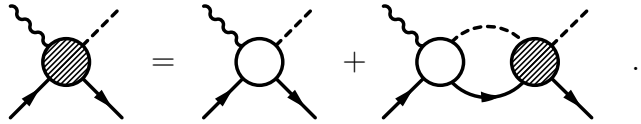


Figure 1: Shown is the electroproduction of mesons on baryons. The empty circle denotes electroproduction at the tree level, whereas the full circles are the full meson-baryon scattering and electroproduction amplitudes. Wavy, dashed and solid lines represent the photon, mesons, and baryons, respectively.

which is illustrated in Figure 1.

The s wave total cross section for the electroproduction of mesons on the nucleon is given by

$$\sigma_{tot} = 8\pi \frac{\sqrt{s}|\mathbf{q}|}{s - M_N^2} (|E_{0+}|^2 + \epsilon_L |L_{0+}|^2), \quad (10)$$

with \mathbf{q} the three-momentum of the meson in the center-of-mass frame and $\epsilon_L = -4\epsilon sk^2(s - M_N^2 + k^2)^{-2}$ where ϵ and k^2 are the virtual photon polarization and momentum transfer, respectively.

3 Results

In this section we will present the results of our calculation. Some of the parameters in our approach are constrained by the octet baryon masses and the $\pi N \sigma$ -term, while others are estimated assuming resonance saturation. The remaining parameters are determined by performing a global fit to available data for meson-proton and photon-proton reactions. This allows us to give predictions for further processes such as the cross sections for $\pi^- p \rightarrow \eta' n$ and η electroproduction.

3.1 Fit to the data

We have performed a global fit to a large amount of data, consisting of meson-proton and photon-proton reactions for values of \sqrt{s} between 1.5 and 2.0 GeV. Our cross sections include only s wave contributions, which are dominant in this energy range for most processes.

Two sample pion-proton cross sections are shown in Fig. 2: Fig. 2.a shows the cross section for the reaction $\pi^- p \rightarrow \eta n$. For momenta p_{lab} below 1 GeV the cross section is dominated by the s wave resonance $S_{11}(1535)$, which is nicely reproduced in our calculation. In Fig. 2.b the results for the reaction

$\pi^- p \rightarrow K^0 \Lambda$ are given. Again the cross section is dominated by s waves, but in this case the main contribution stems from the $S_{11}(1650)$ which is accompanied by a cusp effect due to the opening of the $K\Sigma$ threshold.

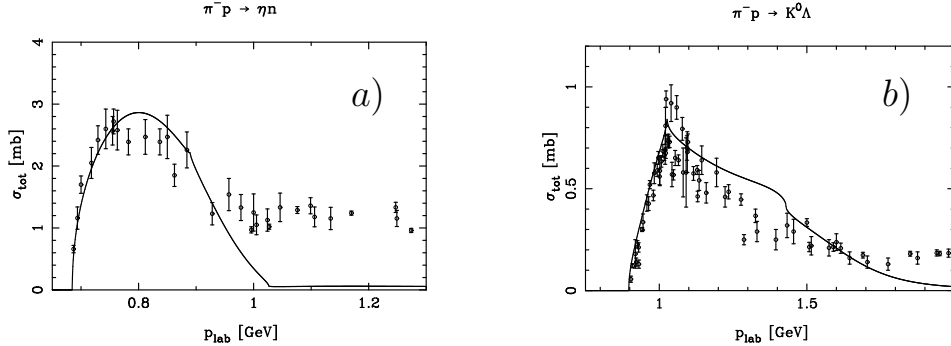


Figure 2: Total cross sections for pion-proton collision processes. The data are taken from [7].

Let us now turn to the photoproduction cross sections which are shown in Fig. 3. We present in Fig. 3.a the η photoproduction data measured at MAMI [8] and ELSA [9] and our fitted result confirms the dominance of the $S_{11}(1535)$, which is responsible for almost the entire cross section in the low-energy region. Results for the reaction $\gamma p \rightarrow K^+ \Lambda$ are given in Fig. 3.b, where at low energies the cross section is dominated by the $S_{11}(1650)$, while p waves become important for E_{lab} energies above 1.1 GeV. Again one observes a cusp effect due to the $K\Sigma$ threshold.

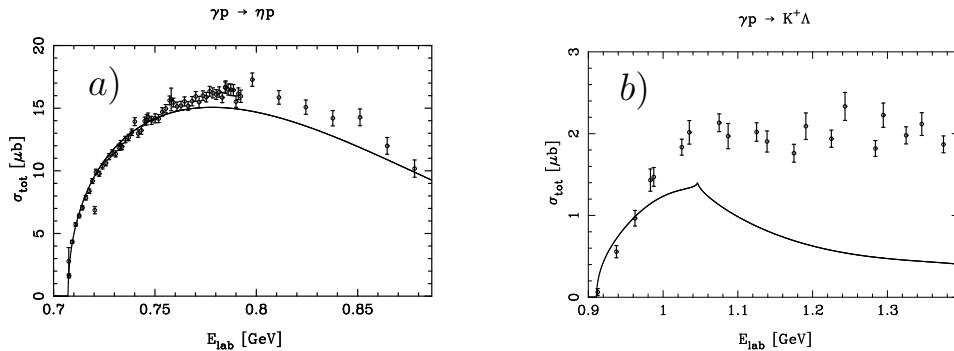


Figure 3: Shown are the total cross sections for η and kaon photoproduction off the proton. The data are taken from [8, 9, 10].

3.2 η' production

We show in Fig. 4.a our result for the reaction $\gamma p \rightarrow \eta' p$, which has been measured at ELSA [2], where the coherent contribution of two resonances, the $S_{11}(1897)$ and $P_{11}(1986)$, was observed. Our formalism is capable of reproducing the appearance of an s wave resonance around 1.9 GeV. Predictions for the cross section of $\pi^- p \rightarrow \eta' n$ are shown in Fig. 4.b.

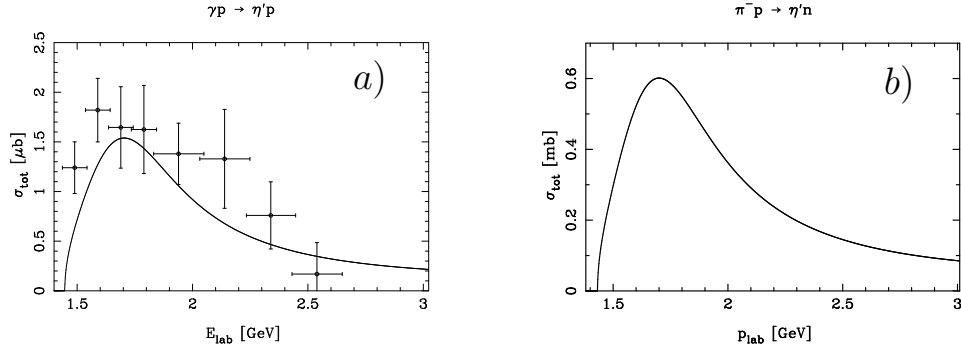


Figure 4: In a) the total cross section for η' -photoproduction off the proton is given and the data are taken from [2]. The total cross section for pion-induced η' -production is shown in b).

3.3 Electroproduction of η mesons

We can furthermore compare our predictions for η electroproduction with available experimental data. We first present our predictions for pointlike hadrons. The η electroproduction on the proton has been measured in detail at CLAS at JLab [11] and the data is shown together with our results in Fig. 5.a.

The invariant momentum transfer Q^2 of the presented data ranges from 0.375 to 0.875 GeV 2 and the applicability of our approach to such high momentum transfers may be regarded as questionable. Nevertheless, we should be able to capture qualitative features of the Q^2 evolution of the cross section, in particular its slow fall-off which is unusual and in sharp contrast, *e.g.*, to the fall given by a nucleon dipole form factor. Our results, although showing less decrease with Q^2 than that of a simple nucleon dipole form factor, produce a faster reduction at low Q^2 than the experimental data, and then flatten at higher momentum transfers.

The composite structure of baryons and mesons will become increasingly important with rising invariant momentum transfers Q^2 . It is therefore natural

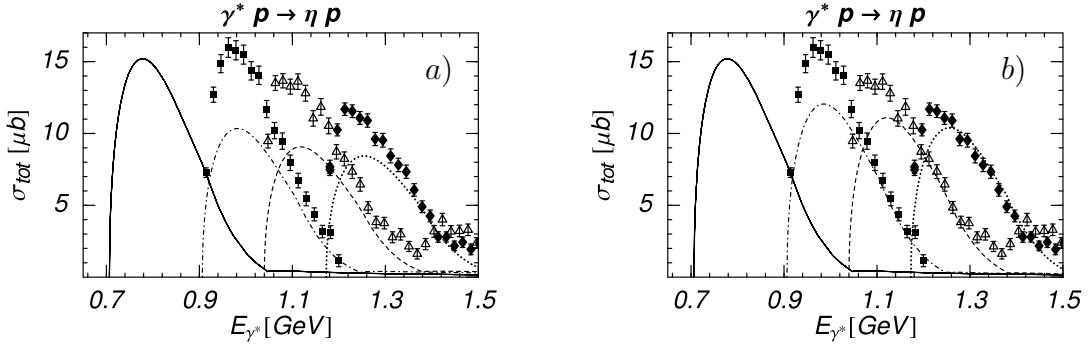


Figure 5: Cross sections for η electroproduction on the proton for various invariant momentum transfers Q^2 without (a) and with (b) transition form factors. The different lines refer to the following values of Q^2 : solid line: photoproduction ($Q^2 = 0$); dash-dotted line and squares: $Q^2 = 0.375$ GeV 2 ; dashed line and triangles: $Q^2 = 0.625$ GeV 2 ; dotted line and diamonds: $Q^2 = 0.875$ GeV 2 . The data with the same Q^2 values are taken from [11], and only statistical errors are shown.

to include form factors in the initial electroproduction potentials B_{0+} and C_{0+} , in order to account for the electromagnetic structure of hadrons. One may be inclined to multiply the potentials by an overall form factor which is the same for all hadrons that interact with the photon (and thus the same for all channels). However, this procedure will also yield smaller cross sections for η electroproduction leading to stronger disagreement with the data. In this case, the inclusion of form factors which accounts for the electromagnetic structure of the baryons and mesons seems to worsen the situation.

In order to model the electromagnetic structure of B_{0+} and C_{0+} , we include monopole form factors $(1 + Q^2/M_\alpha^2)^{-1}$ with mass parameters M_α depending on the outgoing channel α . The results for η electroproduction after including these form factors are given in Fig. 5.b. Surprisingly, the cross sections for η electroproduction are *increased*. This is due to the fact that we employed different form factors for the participating channels and that some of these channels may compensate each other in the final state interactions. In contrast to common belief, the inclusion of form factors can increase the cross section, *e.g.* in η electroproduction, yielding a Q^2 evolution closer to experiment and indicating a hard transition form factor. The usual claim that the hard form factor is counterintuitive to an interpretation of this state as a bound hadronic system is not justified, since within the model the photon couples directly to one of the ground state octet baryons or a meson and only after this initial

reaction the produced meson forms a bound state with the baryon.

We do not expect our results for electroproduction to reproduce precisely the experimental data. Nevertheless, the inclusion of simple form factors for the electroproduction potentials is able to explain qualitatively the slow decrease of the $S_{11}(1535)$ photocoupling.

3.4 Effects of the η'

In this section, we wish to investigate the effects of η - η' mixing and the importance of the $|\eta'N\rangle$ virtual state in our coupled channel formalism. This is done in a two-step procedure: first, η - η' mixing is turned off, and secondly, we eliminate the $|\eta'N\rangle$ channel from the model. In both cases we do not repeat the fit which would actually compensate most of the changes. We are particularly interested in the reaction $\pi^- p \rightarrow K^0 \Lambda$ which exhibits the most prominent $\eta'N$ cusp of all the channels. Omission of both η - η' mixing and the $|\eta'N\rangle$ channel do not lead to substantial differences in the remaining reactions (where the η' is not produced). In Fig. 6 we have chosen to present in addition to $\pi^- p \rightarrow K^0 \Lambda$ the photoproduction process $\gamma p \rightarrow \eta p$, in order to give a measure for the changes in the other channels. For $\pi^- p \rightarrow K^0 \Lambda$ variation in

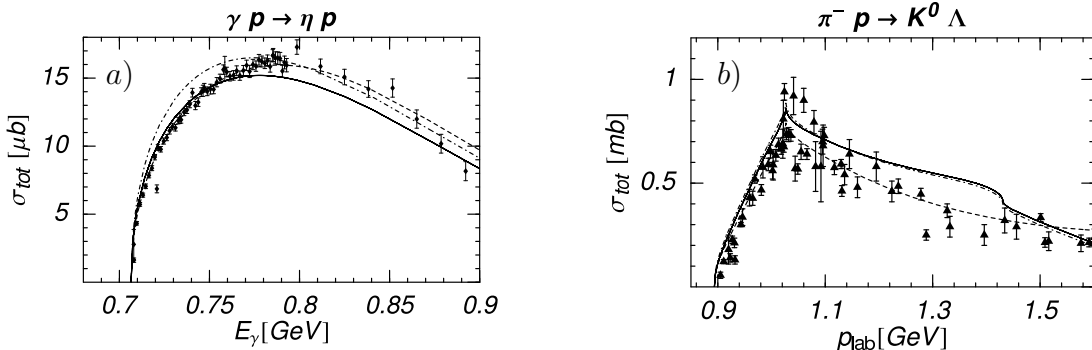


Figure 6: Shown are the differences in the cross sections for $\gamma p \rightarrow \eta p$ and $\pi^- p \rightarrow K^0 \Lambda$ after neglecting η - η' mixing and the $|\eta'N\rangle$ channel in the coupled channel formalism. The solid line is the original result, the dash-dotted line is obtained for vanishing η - η' mixing, and the dashed line refers to the case without the $|\eta'N\rangle$ channel.

η - η' mixing has almost no impact (dash-dotted line), like in most other channels in which the η is not produced as a final particle. Eliminating the $|\eta'N\rangle$ channel makes the $\eta'N$ cusp disappear and lowers the cross section, bringing it to better agreement with the data (dashed line). It suggests that the re-

gion around the $\eta'N$ cusp is overemphasized within our model. This feature may change after the inclusion of p waves, since then a new overall fit to the different reaction channels will lower the s wave contribution reducing the absolute importance of the cusp. For the photoproduction of the η on the proton η - η' mixing plays a slightly more prominent role (dash-dotted line), as the η is produced in the final state. If the $|\eta'N\rangle$ channel is turned off, the changes are again quite moderate (dashed line). Overall we can conclude, that the results for the production of the Goldstone bosons are not modified substantially after omitting the η' which is in accordance with intuitive expectation, since the $|\eta'N\rangle$ channel is much higher in mass than the other channels. We can therefore confirm that it was justified in previous coupled channel analyses to neglect η - η' mixing and treat the η as a pure octet state, see e.g. [12].

Acknowledgement

This work was supported by the Deutsche Forschungsgemeinschaft.

References

- [1] See, *e.g.*, N. Kaiser, P. B. Siegel, and W. Weise, Nucl. Phys. **A594** (1995) 325; M. F. M. Lutz and E. E. Kolomeitsev, Nucl. Phys. **A700** (2002) 193.
- [2] R. Plötzke et al., Phys. Lett. **B444** (1998) 555.
- [3] B. Borasoy, Phys. Rev. D61 (2000) 014011.
- [4] H. Leutwyler, Phys. Lett. **B374** (1996) 163.
- [5] N. Beisert and B. Borasoy, Eur. Phys. J. Bf A11 (2001) 329.
- [6] B. Borasoy, E. Marco, and S. Wetzel, Phys. Rev. **C66** (2002) 055208.
- [7] A. Baldini et al., *Total Cross-Sections for Reactions of High-Energy Particles*, Landolt-Börnstein, New Series, Group I, Vol. 12, Pt. a (Springer, Berlin, 1988).
- [8] B. Krusche et al., Phys. Rev. Lett. **74** (1995) 3736.
- [9] B. Schoch, Prog. Part. Nucl. Phys. **35** (1995) 43.
- [10] M. Q. Tran et al. (SAPHIR Collaboration), Phys. Lett. **B445** (1998) 20.
- [11] R. Thompson et al., Phys. Rev. Lett. **86**, (2001) 1702.
- [12] N. Kaiser, T. Waas, W. Weise, Nucl. Phys. **A612** (1997) 297.